Photoreflectance study of GaAsSb/InP heterostructures

Houssam Chouaib, C. Bru-Chevallier, G. Guillot, H. Lahreche, P. Bove

Photoreflectance study of GaAsSb/InP heterostructures

H. Chouaib,[a] C. Bru-Chevallier, and G. Guillot
Laboratoire de Physique de la Matière, INSA de Lyon (UMR-CNRS 5511), Bâtiment Blaise Pascal, 7 Avenue J. Capelle, 69621 Villeurbanne, France

H. Lahreche and P. Bove
Picogiga, Place M. Rebuffat 91971 Courtaboeuf cedex 7, France

(Received 28 October 2004; accepted 7 November 2005; published online 29 December 2005)

Photoreflectance (PR) spectroscopy experiments are reported on GaAsSb/InP heterostructures. The GaAsSb PR spectrum is studied as a function of temperature and the transition nature is shown to change from Franz-Keldysh oscillations (FKO) at room temperature to a third derivative functional form (TDFF) line shape at low temperatures. Combining both analysis (FKO and TDFF) in the same sample, we derive internal electric field and phase values of the PR transition, together with accurate values for alloy band gap energy on the whole temperature range. Type II interface recombination is shown to reduce photovoltage effects as a function of temperature. FKO are found to appear for a very weak electric field (8 kV/cm) in the GaAsSb/InP heterostructure, contrary to usual observations. This point is discussed in relation with the broadening parameter of the transition. © *2005 American Institute of Physics*. [DOI: 10.1063/1.2142099]

I. INTRODUCTION

Photoreflectance (PR) spectroscopy has been used to characterize semiconductor heterostructures and a number of device structures such as heterojunction bipolar transistors (HBT),[1–4] high electron mobility transistors,[5,6] and quantum well lasers.[7] Because of its derivative-like nature a large number of sharp spectral features can be observed, even at room temperature, and it is possible to determine the energy and broadening parameter of any direct interband transition.[8] For sufficiently high electric fields, the PR spectrum displays an oscillatory behavior, [the so-called Franz-Keldysh oscillations (FKO)] whose period is a direct measure of the internal electric field.

The high speed performance of InP based HBT has been demonstrated in many circuit applications.[9] The ternary III-V semiconductor GaAsSb is a material of interest for the base of HBT[10] realized in the family of GaInAs materials lattice matched to InP. Due to the type II conduction band offsets,[11,12] and to the favorable band alignment of the conduction band at the base-collector junction, a weak saturation voltage is expected. Very high *p*-type doping levels using carbon in GaAsSb (2×10^{20} cm^{-3}) have also been reported.[13]

This article reports a PR study of GaAsSb/InP heterostructures in the temperature range between 8 and 300 K. The nature of PR transitions is analyzed as a function of temperature. Both analysis third derivative functional form (TDFF) and FKO are used in order to evaluate the GaAsSb alloy band gap energy in the whole temperature range as well as the internal electric field in the heterostructure.

II. EXPERIMENTAL DETAILS

The samples were grown by molecular beam epitaxy on InP substrates and their structures and band diagrams are drawn in Fig. 1. An InP layer is deposited on a Si doped InP substrate, which is either silicon doped in sample A (3×10^{18} cm^{-3}), or nonintentionally doped (nid) in sample B residual *n*-type 10^{16} cm^{-3}. A nid GaAsSb layer is then deposited on top of the InP buffer layer. Associated high resolution x-ray diffraction (HRXRD) spectra give the following Sb composition for the GaAsSb alloys: 45.7% in sample A and 50.4% in sample B. HRXRD measurements give access to the alloy lattice parameter, the antimony composition being extracted assuming a fully strained alloy.

In the photoreflectance experiments, the probe beam is supplied through a monochromator from a halogen lamp, and the optical modulation of the built-in electric field is realized by a 20 mW HeNe laser which is chopped at 320 Hz. The intensity of the modulating beam is controlled by neutral density filters. The reflectance signal is detected by an InGaAs photodiode. The modulated part of the reflected signal is extracted using a conventional lock-in technique. The PR spectra are recorded in the 8–300 K temperature range, the samples being mounted in a cold finger variable temperature cryostat.

III. RESULTS

The PR spectra recorded in samples A and B at 300 K are displayed in Fig 2. Both of them exhibit oscillations above the GaAsSb band gap: nine oscillations for sample A and four oscillations for sample B. These FKO are related to the internal electric field in the GaAsSb layer. It is worth noting that the PR transition intensity in sample A is much stronger than in sample B. This will be discussed in the following section.

A wide and small PR transition is arising at high energy (about 1.1 eV) in sample A (Fig. 2): it is attributed to the spin-orbit splitting of the GaAsSb valence band $E_0+\Delta_0$.

In Fig. 3 are plotted the PR spectra of both samples at temperatures varying between 8 and 300 K. PR spectra ex-

[a]Author to whom correspondence should be addressed; electronic mail: houssam.chouaib@insa-lyon.fr

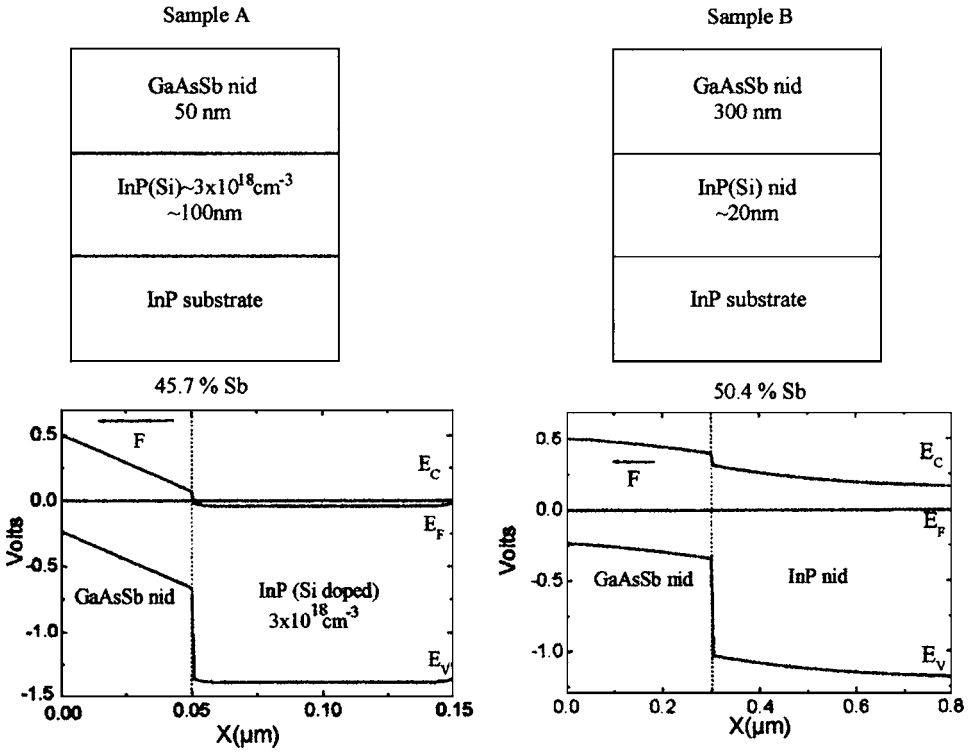

FIG. 1. Sample structures (A and B) and their corresponding band diagram calculated from a simple Poisson equation model.

hibit FKO in the whole temperature range, except for sample B below 100 K where the nature of the transitions moves from FKO to the low electric field TDFF of the unperturbed dielectric function. As expected, the energy gap is found to decrease as the temperature is increased. The PR experimental results are analyzed and discussed in the next section.

IV. PHOTOREFLECTANCE ANALYSIS

Photoreflectance can be classified into three categories: low, intermediate, and high field regimes, depending on the relative strengths of the electro-optic energy as compared to the broadening of the PR transition. In the low electric field regime, the modulation $\Delta\varepsilon$ of the dielectric function ε has a line shape that is the TDFF of the unperturbed optical function.[14]

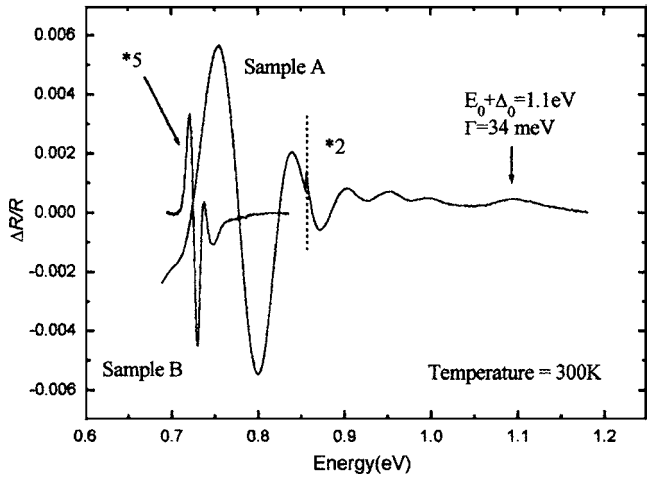

FIG. 2. PR spectra of samples A and B at room temperature.

Differential changes in the reflectivity R are related to the perturbation of the complex dielectric function $\Delta\varepsilon$ by the Seraphin equation:[15]

$$\frac{\Delta R}{R} = a\Delta\varepsilon_1 + b\Delta\varepsilon_2, \tag{1}$$

where a and b are the Seraphin coefficients and ε_1 and ε_2 are the real and imaginary parts of the dielectric function ε. In most cases, near the fundamental gap of bulk materials, coefficient b is very small and the second term in Eq. (1) can be neglected in such a way that $\Delta R/R$ is proportional to the modulation of the real part of the dielectric function $\Delta\varepsilon_1$.

If the form of ε_1 is a generalized Lorentzian form, which is the case for homogeneous broadening, $\Delta R/R$ takes a particularly simple form:[16]

$$\frac{\Delta R}{R} = (\hbar\theta)^3 \mathrm{Re}[Ae^{i\Phi}(E - E_G + i\Gamma)^{-n}], \tag{2}$$

where A is the amplitude, Φ is a phase angle, n is an exponent coefficient which depends on the type of the critical point of energy band structure, and $\hbar\theta = (q^2F^2\hbar^2/2\mu)^{1/3}$ is the electro-optic energy with F the electric field and μ the reduced effective mass, q and h are, respectively, the elementary charged and Planck's constant. By fitting PR data, the band gap energy E_G and broadening parameter Γ are extracted. The line shape factor is independent on the modulating field F in the low-field regime, and depends only on the shape of the unperturbed dielectric function.

But in the event that the low-field criterion ($\hbar\theta \ll \Gamma$) is not satisfied, in the intermediate field regime, $\Delta\varepsilon$ exhibits FKO. From these FKO, it is possible to evaluate the built-in electric field F_{dc} and the band gap energy E_G. The extrema in FKO are given by:[17]

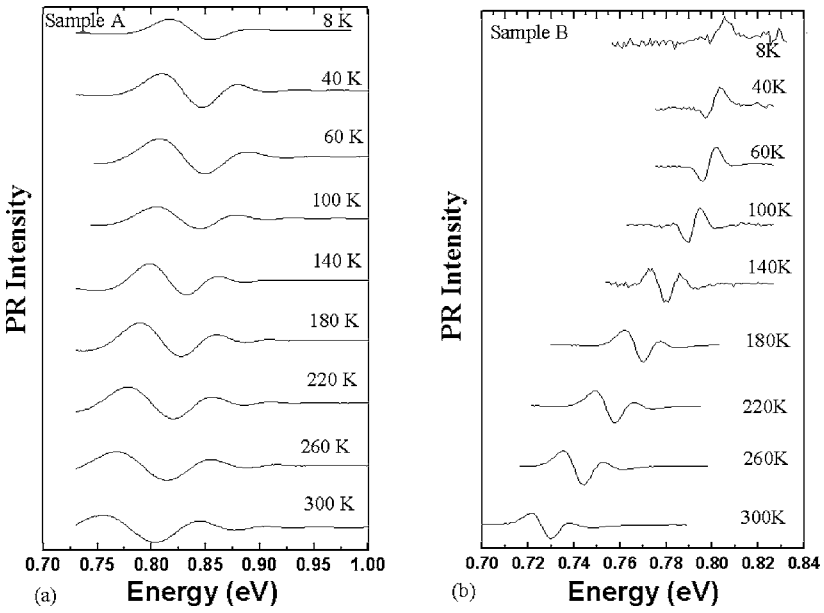

FIG. 3. Evolution of PR spectra versus temperature in (a) sample A and (b) sample B.

$$m\pi = \frac{4}{3}\left(\frac{E_m - E_G}{\hbar\theta}\right)^{3/2} + \psi, \tag{3}$$

where m is the extremum index, E_m is the PR extremum energy, and ψ is an arbitrary phase factor. From Eq. (3), it follows that

$$E_m - E_G = \hbar\theta\left(\frac{3}{4}(m\pi - \psi)\right)^{2/3}. \tag{4}$$

A plot of E_m versus $\left(\frac{3}{4}(m\pi-\psi)\right)^{2/3}$ will yield a straight line with slope $\hbar\theta$ which contains the electric field F. The intercept with vertical axis gives the band gap energy E_G providing that the phase ψ is known. However this phase does not have a simple interpretation, and though Aspnes[14] previously proposed that ψ could be related to the dimensionality d of the critical point following: $\psi=\pi(d-1)/4$, such a formula is not universal and Eq. (4) cannot generally be used to get an accurate value of the band gap energy E_G. Indeed, the intercept with vertical axis (E_G) does depend a lot on the phase value, and the determination of band gap energy from FKO is not straightforward.

V. DISCUSSION

Figure 4 displays the PR spectrum of sample B recorded at 60 K (squares), together with the fitting curve (solid line) to a TDFF [Eq. (2)]. The fitting parameters, gap energy E_G and broadening parameter Γ are deduced: E_G=0.799 eV, Γ =4.5 meV at 60 K. The same treatment is also performed at lower temperatures.

At higher temperatures in sample B [Fig. 3(b)], the PR transitions can no more be fitted by TDFF as high energy maxima are arising. They are attributed to FKO oscillations. The internal electric field F and band gap energy E_G are determined following the method described previously, plotting the energy extrema E_m versus a function of m [as illustrated in Fig. 6(a)] for sample B at 300 K. It is worth noting that the four energy maxima are straight aligned: this confirms our assumption that the PR spectra of sample B at high temperatures have a FKO nature. In ternary alloys gap, the exploitation of FKO using Eq. (4) requires the determination of phase ψ. To check its influence on gap energy and electric field values, we varied ψ between $-\pi$ and π and we concluded that the major effect is to change the vertical axis intercept, that is band gap energy E_G. No significant effect is detected on the electric field value. Next, we *a priori* assume that phase ψ does not depend a lot on the temperature, following previous studies[4] which have shown that it essentially depends on optical interferences, which hardly depend on temperature.

In sample B, the alloy gap energy can be determined using both methods: FKO and TDFF. We take advantage of this observation to derive the accurate value of phase ψ, following the above-mentioned assumptions. ψ is chosen in such a way that the determination of gap energy from both methods (FKO and TDFF) gives a correct evolution of E_G versus temperature. Choosing ψ equal to 0.8π in sample B, the evolution of E_G versus temperature does follow the usual Varshni empirical relationship[18] as shown in Fig. 5:

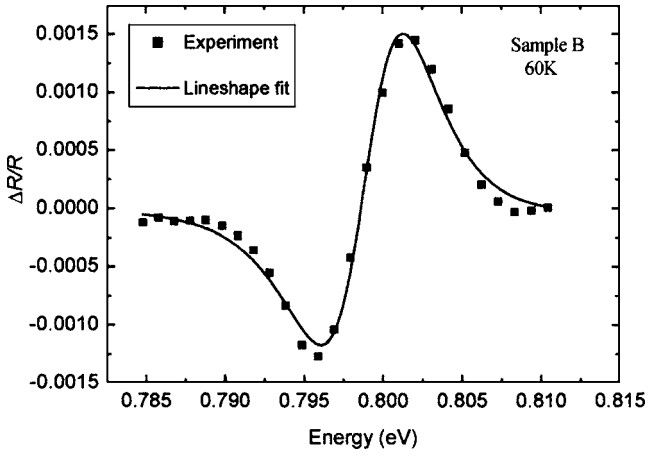

FIG. 4. PR spectrum of sample B at 60 K (dotted curve). TDFF fit using Eq. (2) (solid line).

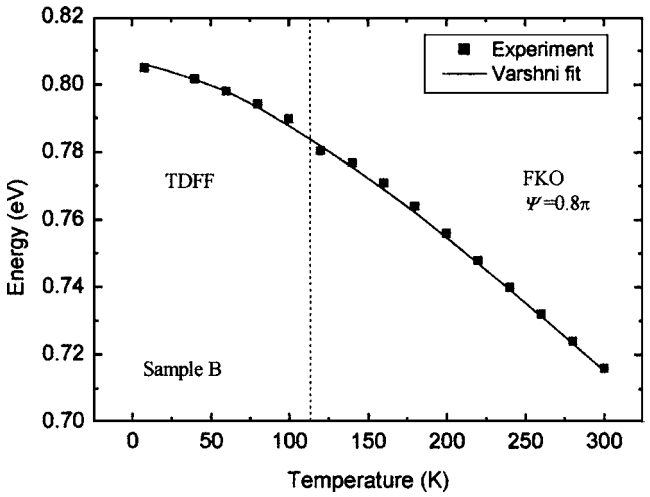

FIG. 5. Temperature dependence of the GaAsSb alloy band gap in sample B (squares extracted from FKO and TDFF theory). Fit to Varshni equation (solid line).

$$E_G(T) = E_G(0) - \frac{\alpha T^2}{\beta + T}. \tag{5}$$

The gap energy at 0 K, $E_G(0)$ and the empirical parameters α and β are, respectively, determined equal to 0.806 ± 0.003 eV, $(4.0 \pm 0.1) \times 10^{-4}$ eV K^{-1}, and 143 ± 18 K in sample B. We check *a posteriori* our previous assumption regarding the independence of ψ on temperature.

From the slope of the straight line ($\hbar\theta_B$) and taking the effective mass value $\mu = 0.042\, m_0$ (Ref. 19) in antimonide alloys, the electric field value is deduced in sample B ($F_B = 8$ kV/cm) at 300 K [Fig. 6(a)]. This experimental value is compared with results obtained from a computer simulation of the band structure using a one-dimensional Poisson equation solver: the maximal theoretical electric field at the interface in such a sample is found to be approximately 7 kV/cm. A good agreement is achieved between theory and experiment.

As previously noticed, the nature of PR line shape in sample B [Fig. 3(b)] is changing from FKO to TDFF as temperature is decreased from 300 down to 10 K. This electric field change is due to the photovoltage effects. Indeed, the optical measurement involves the use of a pump beam which introduces a photovoltage phenomenon[20] which decreases the internal electric field (Fig. 7). This decrease is due to the creation of electron hole pairs which are separated by the internal electric field. This mechanism is very significant at low temperature where the thermoionic effects—which tend to reduce the photovoltage effects—decrease.

In the case of sample A, we cannot use the same method to derive the phase value for FKO analysis, as PR spectra exhibit FKO on the whole temperature range, and no TDFF analysis can be performed at any temperature. However, the gap energy in sample A at 300 K is higher than sample B by about 10 meV. We conclude this from HRXRD experiments performed on both samples which give an Sb concentration 5% lower in sample A than in sample B and the PL study previously performed in the same structures.[21] Therefore, we use this bandgap value at 300K to determine the phase ψ to

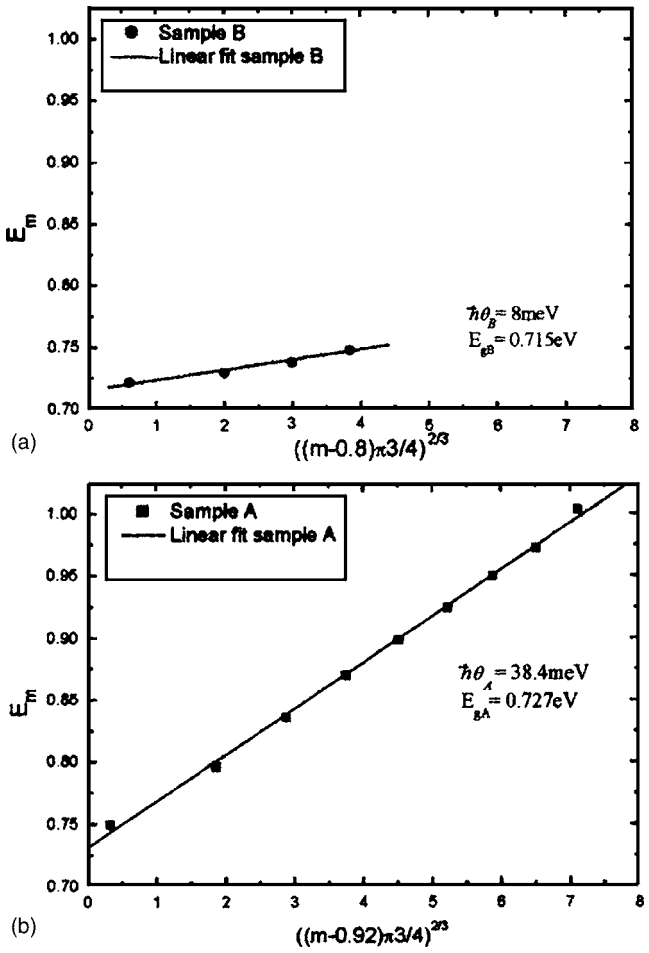

FIG. 6. PR transition energy E_m (a) as a function of $((m-0.8)\pi^*3/4)^{2/3}$ in sample B (m: FKO index) and (b) as a function of $((m-0.92)\pi^*3/4)^{2/3}$ in sample A.

use in the FKO analysis of sample A in the whole temperature range. Taking ψ equal to 0.92π the bandgap energy evolution with temperature in sample A is plotted in Fig. 8 together with the fit to Varshni equation. Parameters $E_G(0)$, α and β are respectively determined equal to 0.818 ± 0.003eV, (3.9 ± 0.1) 10^{-4}eV.K^{-1}, and 140 ± 14K in sample A. Recently,

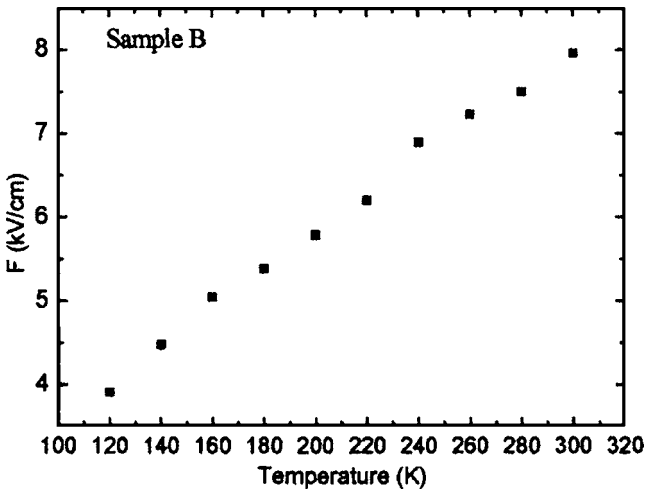

FIG. 7. The temperature dependence of the measured electric field in sample B.

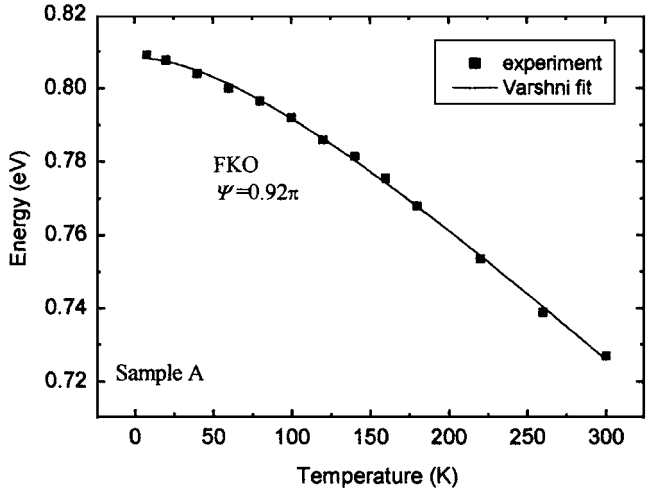

FIG. 8. Temperature dependence of the GaAsSb alloy band gap in sample A. Fit to Varshni equation (solid line).

it has been found that the phase of FKO is strongly sensitive to the total layer thickness over the interface associated with the FKO.[4] Our results confirm these predictions. The difference in the FKO phases between samples A and B is attributed to the difference in the GaAsSb layer thickness.

The high energy transition which appears in the room temperature PR spectrum of sample A (Fig. 2) was previously attributed to the split-off valence band. The transition energy and broadening parameter Γ are determined using a fit to the TDFF lineshape: $E_0+\Delta_0=1.08$eV, $\Gamma=34$meV at 300K. Figure 9 gives the $E_0+\Delta_0$ energy evolution with temperature, together with the fit to Varshni equation. Parameters $E_G(0)+\Delta_0(0)$, α and β are respectively determined equal to 1.155 ± 0.0006 eV, 0.00154 ± 0.0005 eV.K^{-1}, and 1532 ± 600K

Using the phase value 0.92π and the same effective mass value than in sample B, the internal electric field at 300K is found to be $F_A=90$kV/cm in sample A (Fig. 6(b)). The strong difference in the electric field values in samples A (90kV/cm) and B (8kv/cm) arises from their different structure. Sample A can be considered as a so-called UN$^+$ structure[17] (an undoped GaAsSb layer on a highly n-type doped InP layer), in which the electric field is assumed to be constant, completely determined by the Fermi level pinning position at the GaAsSb surface and the thickness of the undoped layer.[22] Assuming a surface Fermi level pinning at 220meV above the valence band,[23] the resolution of 1D Poisson equation in the sample structure yields an electric field value of 90kV/cm in good agreement with the experimental value. The strong difference between the internal electric field values measured in both samples is responsible for the strong difference in PR transition amplitude (Fig. 2) as previously noticed.

It is worth noting that the evolution of electric field versus temperature in many samples of similar structure (like sample A) shows an anomalous behavior, different from what is classically described in the literature when the photovoltage effects[20] are governed by a simple thermoionic effect. Actually, the electric field does not vary a lot with temperature in sample A as previously reported (Figs. 8–10).[21–23]

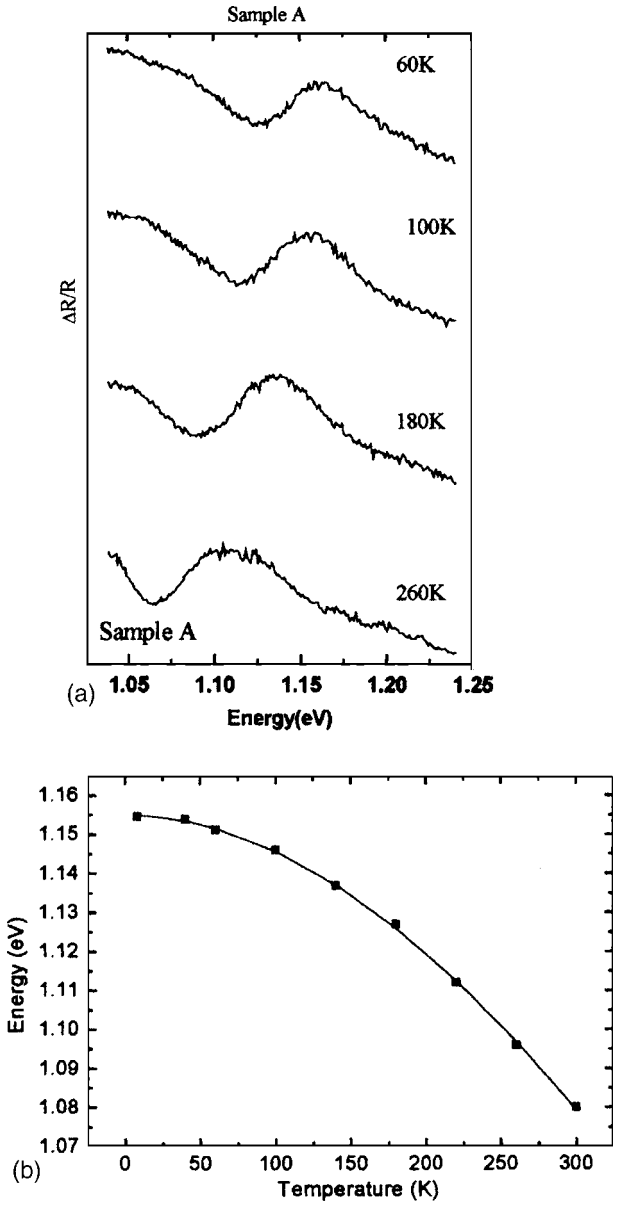

FIG. 9. (a) PR spectra of the split-off valence band transition at different temperature (sample A). Evolution of the transition energy versus temperature. (b) Solid line is a fit to Varshni equation.

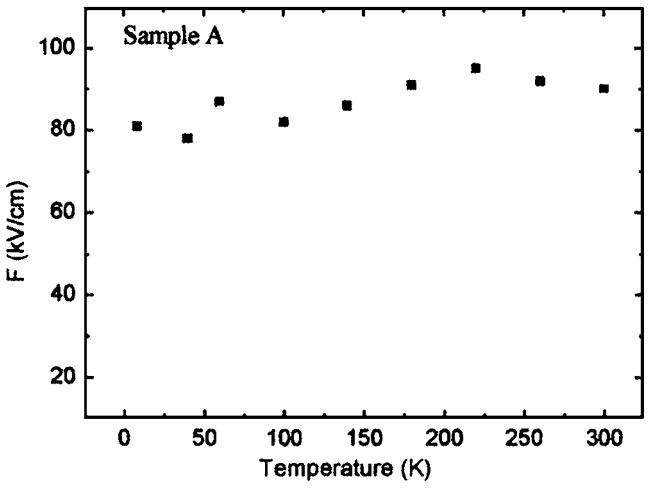

FIG. 10. The temperature dependence of the measured electric field in sample A.

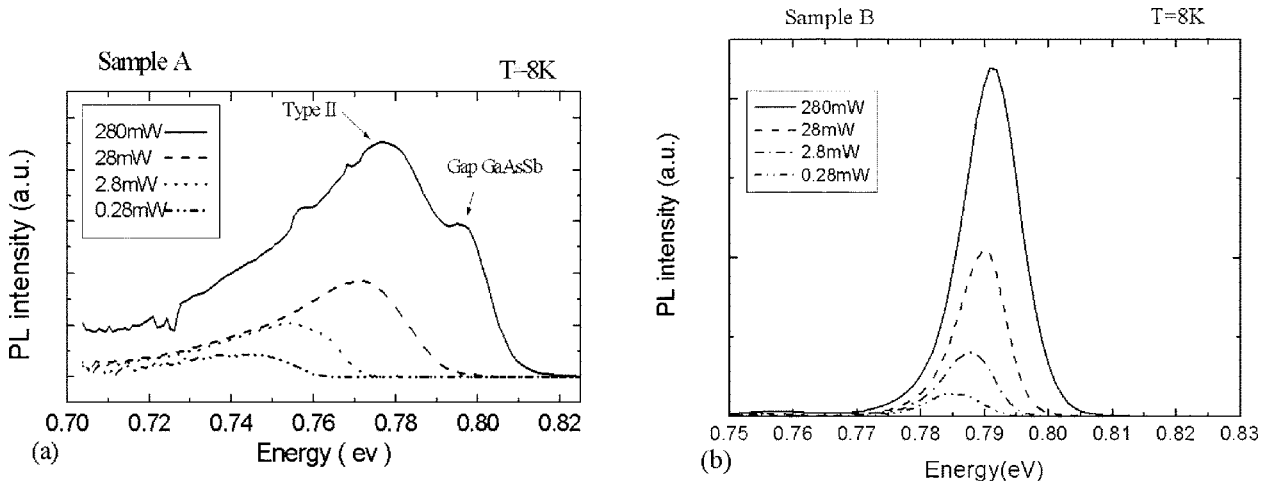

FIG. 11. (a) PL evolution of sample A (b) and of sample B according to the excitation power.

We tentatively attribute this nonclassical behavior to the type II nature of the heterostructures (Fig. 1). Indeed, the photovoltage generated by the modulation light is determined classically without taking account of the recombination phenomena at the interface. In type II heterostructures, the recombination current in the depletion region is relatively high, and the carriers at the interface have a very low lifetime. The amplitude of the spatially indirect type II luminescence of electrons localized in InP and holes in the GaAsSb is usually measured by photoluminescence.[11,12] Figure 11 shows the low temperature PL spectra of both samples A and B at different excitation densities. By increasing the excitation density by a factor of 1000, we observe for sample A, a very strong shift of 40 meV toward high energy. Such large injection-dependent energy shifts have been reported for spatially indirect type II recombination of electrons and holes in other material systems and also in GaAsSb/InP.[11,12] The energy shift comes from the band-bending effect near the interfaces in the high laser excitation region. The reason why we do not see any type II recombination in B sample, is twofold. First the thickness layer is much larger than in sample A. Second, the subjacent InP layer is nonintentionally doped in sample B and therefore decreases the density of electrons available for type II recombination in this sample. We assume that in samples which present a strong type II interface recombination, the internal electric field does not depend a lot on the temperature as shown in Fig. 10. Further work is under way to confirm this assumption, and will be reported later on.

Finally, we would like to emphasize that in sample B, FKO do appear even for a very weak internal electric field (8 kV/cm), although the FKO theory is a so-called intermediate electric field theory, that is when the low field criterion ($\hbar\theta \ll \Gamma$) is not satisfied as described in Sec. IV. At 60 K Γ is found to be 4.5 meV. As temperature is increased, Γ is supposed to increase due to phonon interactions. However, as FKO are still present at 300 K, this means that Γ never becomes much larger than 8 meV at 300 K. This is a proof for a rather weak phonon coupling in such antimonide alloys.

VI. CONCLUSION

In conclusion, we have performed a PR investigation of GaAsSb/InP heterostructures. Taking into account the whole temperature evolution, we were able to accurately derive the phase value to use in FKO analysis, and extract accurate values of antimonide alloy band gap in the whole temperature range, as well as the electric field F at the surface of both samples. The temperature evolution of the alloy band gap was adjusted using empirical Varshni law. The evolution of electric field versus temperature is shown to be strongly influenced by type II interface recombination. The observation of FKO at 300 K for a rather low internal electric field is a proof for weak phonon coupling in GaAsSb alloys.

ACKNOWLEDGMENT

This work was supported by the Réseau National de Recherches en Télécommunications (RNRT-MELBA project).

[1] C. J. Lin and Y. S. Huang, J. Appl. Phys. **90**, 4565 (2001).
[2] Y. S. Huang, W. D. Sun, L. Malikova, Fred H. Pollak, T. S. Low, and James S. C. Chang, Appl. Phys. Lett. **73**, 1215 (1998).
[3] C. Monier and A. G. Baca, Appl. Phys. Lett. **81**, 2103 (2002).
[4] H. Takeuchi, Y. Yamamoto and M. Nakayama, J. Appl. Phys. **96**, 1967 (2004).
[5] G. Sek, J. Misiewicz, M. Kaniewska, K. Reginski and J. Muszalski, Vacuum **48**, 283 (1997).
[6] D. Y. Lee, J. S. Kim, D. L. Kim, K. H. Kim, J. S. Son, I. S. Kim, B. K. Han, and I. H. Bae, J. Cryst. Growth **243**, 66 (2002).
[7] R. Kudrawiec, G. Sek, K. Ryczko, J. Misiewicz, and A. Forchel, Mater. Sci. Eng., B **102**, 331 (2003).
[8] F. H. Pollak, in *Handbook on Semiconductors*, edited by M. Balkanski (North-Holland, New York, 1994).
[9] H. Kamitsuna, Y. Matsuoka, S. Yamahata, and K. Kurishima, Tech. Dig. GaAs IC Symp. IEEE, 1995, p. 185.
[10] M. W. Dvorak, C. R. Bolognesi, D. J. Pitts, and S. SP Watkins, IEEE Electron Device Lett. **22**, 361 (2001).
[11] M. Peter, N. Herres, F. Fuchs, K. Winkler, K.-H. Bachem, and J. Wagner, Appl. Phys. Lett. **74**, 410 (1999).
[12] J. Hu, X. G. Xu, J. A. H. Stotz, S. P. Watkins, A. E. Curzon, M. L. W. Thewalt, N. Matine, and C. R. Bolognesi, Appl. Phys. Lett. **73**, 2799 (1998).
[13] S. P. Watkins, O. J. Pitts, C. Dale, X. G. Xu, M. W. Dvorak, N. Matine and C. R. Bolognesi, J. Cryst. Growth **221**, 59 (2000).
[14] D. E. Aspnes, Phys. Rev. B **10**, 4228 (1974).
[15] B. O. Seraphin and N. Bottka, Phys. Rev. **145**, 628 (1966).
[16] F. H. Shen and F. H. Pollak, Phys. Rev. B **42**, 7097 (1990).

[17]H. Shen and M. Dutta, J. Appl. Phys. **78**, 2151 (1995).
[18]Y. P. Varshni, Physica (Amsterdam) **34**, 149 (1967).
[19]*Handbook Series on Semiconductor Parameters*, edited by M. Levinshtein, S. Rumantsev, and M. Shur (World Scientific, Singapore, 1999), Vol. 2.
[20]M. H. Hecht, Phys. Rev. B **41**, 7918 (1990).
[21]H. Chouaib, C. Bru-Chevallier, T. Benyattou, H. Lahreche, and P. Bove Mater. Res. Soc. Symp. Proc. **799**, 193 (2004).
[22]H. Shen, M. Dutta, L. Fotiadis, P. G. Newman, R. P. Moerkirk, W. H. Chang, and R. N. Sacks, Appl. Phys. Lett. **57**, 2118 (1990).
[23]C. Bru-Chevallier, H. Chouaib, J. Arcamone, T. Benyattou, H. Lahreche, and P. Bove, Thin Solid Films **450**, 151 (2004).